LRO-LAMP DETECTION OF GEOLOGICALLY YOUNG CRATERS IN LUNAR SOUTH POLE PERMANENTLY SHADED REGIONS. Kathleen E. Mandt[1], Thomas K. Greathouse[1], Kurt D. Retherford[1], G. Randall Gladstone[1], Andrew P. Jordan[2], Myriam Lemelin[3], Steven D. Koeber[4], Ernest Bowman-Cisneros[4], G. Wesley Patterson[5], Mark Robinson[4], Paul G. Lucey[3], Amanda R. Hendrix[6], Dana Hurley[5], Angela M. Stickle[5], Wayne Pryor[7], [1]Southwest Research Institute, Space Science & Engineering, PO Drawer 28510, San Antonio, TX 78228 kmandt@swri.org, [2]Institute for the Study of Earth, Oceans, and Space, University of New Hampshire, Durham, New Hampshire, USA, [3]Hawai'i Institute of Geophysics and Planetology, University of Hawai'i at Mānoa, Honolulu, HI 96822, [4]Arizona State University, Tempe, AZ, [5]Johns Hopkins University Applied Physics Laboratory, Laurel, MD, [6]Planetary Science Institute, Tucson, AZ 85719, [7]Central Arizona College, Coolidge, AZ 85128.

Introduction: Geologically young, or "fresh", craters provide an important opportunity to calibrate space weathering processes [1,2]. Permanently shaded regions (PSRs) of the Moon are difficult to study, but are of great scientific and exploration interest because of their expected ability to trap and retain volatiles for billions of years [3,4]. Unfortunately, little is known about their surface properties or space weathering rates compared to other regions of the Moon. We describe here the detection of two geologically young craters within south polar PSRs using maps of the Lyman-α (121.57 nm) albedo of their interiors. These maps were produced using data taken by the Lyman Alpha Mapping Project (LAMP), a far-ultraviolet (FUV) imaging spectrograph [5] on the NASA Lunar Reconnaissance Orbiter (LRO) [6]. This work demonstrates a new method for detecting fresh craters on the Moon and provides observations that are useful for studying space weathering processes within PSRs.

Space Weathering: Space weathering occurs through several processes, including impact gardening [7], solar wind sputtering [8] and possibly dielectric breakdown [9,10]. Impact gardening is the turnover of regolith by micrometeoroid impacts, while exposure to the solar wind sputters atoms from the surface that are redeposited as a coating on the surrounding regolith. Dielectric breakdown, a proposed process that may be unique to the PSRs, occurs when large solar energetic particle events cause dielectric breakdown in locations where cold temperatures greatly lengthen the regolith's electrical discharging timescale. If effective in the PSRs, dielectric breakdown could increase surface porosity, among other effects [9,10].

Fresh craters provide a snapshot in time of space weathering conditions and are valuable tools for evaluating the influence of space weathering on lunar regolith. They are brighter at visible wavelengths due to the exposure of material not previously subjected to space weathering [1,2] and have high Circular Polarization Ratios (CPR) due to increased surface roughness at centimeter to decimeter scale [11,12]. Near UV (300-400 nm) observations show that space weathering causes the spectrum of the regolith to mature faster at UV wavelengths than at visible or infrared wavelengths (VNIR – 400-1400 nm) [1], which means that fresh craters detected in the FUV (100-200 nm) could be significantly younger than those identified as fresh in the VNIR. Therefore, the use of starlight and skyglow illumination by LRO-LAMP to map the PSRs [5,13] provides a unique tool for detecting fresh craters in these difficult-to-study regions.

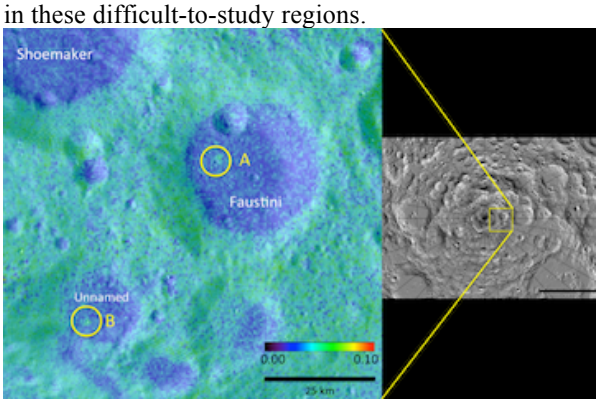

Figure 1: LAMP Lyman-α albedo overlaid on a LOLA shaded relief map. The circles surrounding craters A & B have a radius of 3 km and are centered on the craters (inset). LOLA shaded relief map of the lunar south polar region (area south of 80° S latitude) produced using the JMoon beta tool (http://jmars.asu.edu/node/2055). Lines of latitude and longitude are shown for every 10°. The box indicates the region of focus.

Mapping the South Pole in Ultraviolet: The LAMP team has created a local area mapping software package to evaluate targeted regions of the moon. This tool produces data cubes of up to 20°x20° degree (latitude and longitude) spatial coverage with square surface sampling as small as 250 m x 250 m. These data cubes consist of surface maps at 69 independent wavelengths (55.57-193.57 nm at 2 nm resolution) covering the entirety of the LAMP bandwidth.

Fig. 1 illustrates the average albedo of the South polar region of the moon at Lyman-α wavelengths. The PSRs are the portions of the map that have a lower UV albedo than their surroundings, likely due to higher porosity of the upper 25-100 nm of regolith within the PSRs [13]. For this study we focus on two small, anomalously bright regions (A & B) within Faustini

and Slater craters that otherwise exhibit low LAMP Lyman-α albedo [14]. These bright regions correlate with what appears to be the ejecta blankets of small (<2km) craters. The Lyman-α albedos of the polar region south of 80° latitude, south pole PSRs and the two bright regions are illustrated in Fig. 2 along with their modeled porosity [13, 14]. It is clear from this figure that the Lyman-α albedos of the ejecta blankets of craters A & B are much higher than their surrounding PSRs, suggesting a 40-50% decrease in their porosity compared to the PSR in general. Moreover, the ejecta blanket Lyman-α albedos are higher than the average albedo for the south polar region, implying a porosity that is up to 5% lower than the south pole region.

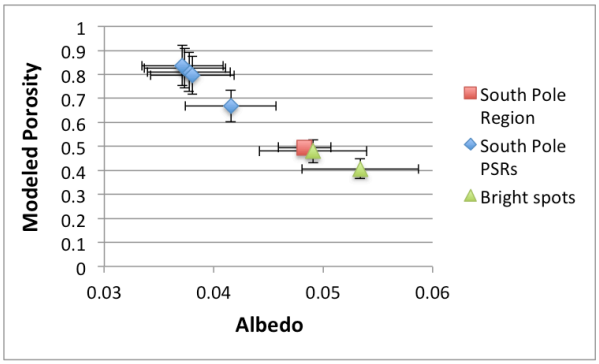

Figure 2: LAMP Lyman-α albedo and modeled porosity. Error bars for the albedo are based on counting statistics, which are then propagated to the modeled porosity value.

Comparison with other LRO datasets: When we compare LAMP observations with Lunar Orbiter Laser Altimeter (LOLA) [15] shaded relief maps we observe that crater A's ejecta blanket appears to extend to the right and above the crater while the ejecta blanket of crater B surrounds the crater symmetrically. Craters A & B can be seen in scattered light images taken by the Lunar Reconnaissance Orbiter Camera (LROC - Figs. 3a & 3b) [16], but it is difficult to tell if the visible reflectance of their ejecta blankets is different from other craters within the PSRs. At high contrast, the rims of the craters appear sharp, as is common for fresh craters.

The annual average temperature (Fig. 3c), measured by LRO Diviner [17] shows that the average temperature for crater A is not different from the surrounding PSR, but that crater B may be slightly cooler than the surrounding PSR. A very distinctive property of these craters is the elevated CPR for the ejecta blankets (Fig. 3d) measured by Mini-RF [18]. Crater A appears to have a more extensive ejecta blanket in the CPR map than in the LAMP Lyman-α albedo map, while the ejecta blanket of crater B looks similar in both the CPR and Lyman-α albedo maps.

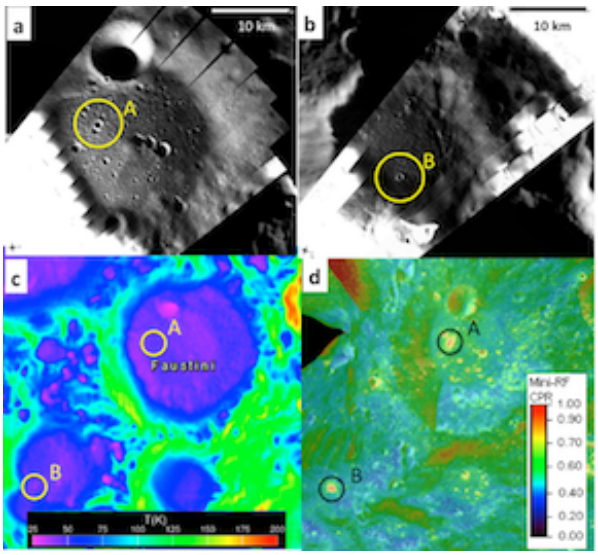

Figure 3: (a) LROC composite image of the interior of Faustini. (b) LROC composite image of the interior of Slater crater. (c) Annual average temperature measured by Diviner (d) Mini-RF CPR of the two PSRs and the surrounding area. As in Fig. 1, craters A & B are identified with circles drawn to have a radius of 3 km and centered on the craters

Estimating the crater ages: Processes that transport very small regolith grains will deposit μm-scale layers of highly porous regolith that eliminate the evidence observed by LAMP for a fresh crater. The evidence for increased surface roughness would remain until impact gardening reduces the surface roughness observed by Mini-RF. We estimate an upper limit of 420 Myr for the age of both craters based on possible timescales for grain transport on the lunar surface. The observed extent of the Mini-RF discontinuous halo [11] for craters A & B in radar brightness gives a narrower age limit of 75-420 Myr for crater A and an approximate age of 16 Myr for crater B.

References: [1] Denevi et al. (2014) *JGR, 119*, 976-997. [2] Robinson et al. (2015) *Icarus, 252*, 229-235. [3] Watson et al. (1961) *JGR, 66*, 1598-1600. [4] Paige et al. (2010a) *Science, 330*, 479. [5] Gladstone, G. R. et al. (2010) *SSRv, 150*, 161–181. [6] Chin et al. (2007) *SSRv, 129*, 391-419. [7] Arnold (1975) *Moon, 13*, 159-172. [8] Hapke (1973) *Moon, 7*, 342-355. [9] Jordan et al. (2014) *JGR, 119*, 1806-1821. [10] Jordan et al. (2015) *JGR, 120*, 210-225. [11] Bell et al. (2012) *JGR, 117*, E00H30. [12] Spudis et al. (2013) *JGR, 118*, 2016-2029. [13] Gladstone, G. R. et al. (2012) *JGR, 117*, E00H04. [14] Mandt et al. (2015) *Icarus,* in press. [15] Smith, D. E. et al. (2010) *SSRv, 150,* 209-241. [16] Robinson et al. (2010) *SSRv, 150*, 81-124. [17] Paige et al. (2010b) *SSRv, 150*, 125-160. [18] Nozette et al. (2010) *SSRv, 150*, 285-302.